Magnetochemical Properties and Reactions of Vanadium(III) Thiolate Complexes: Preparation of (NEt₄)₃[V₃Cl₆(edt)₃] and Mixed-Valence (NEt₄)[V₂(edt)₄] (edt = Ethane-1,2-dithiolate)

Joe R. Rambo, Stephanie L. Castro, Kirsten Folting, Stuart L. Bartley,[1] Robert A. Heintz,[1] and George Christou*

Department of Chemistry and Molecular Structure Center, Indiana University, Bloomington, Indiana 47405-4001

Received June 17, 1996[⊗]

Reactions of the previously reported dinuclear vanadium(III) thiolate anion $[V_2(edt)_4]^{2-}$ (edtH$_2$ = ethane-1,2-dithiol) are described. Treatment of (NEt$_4$)$_2$[V$_2$(edt)$_4$] (**1**) in MeCN with equimolar (C$_{12}$H$_8$S$_2$)BF$_4$ (C$_{12}$H$_8$S$_2$$^+$ = the thianthrenium radical cation) results in a one-electron oxidation and isolation of the V^{III},V^{IV} complex (NEt$_4$)-[V$_2$(edt)$_4$] (**2**). The same product can also be obtained by controlled-potential electrolysis of **1** at −0.20 V *vs* Ag/AgCl. Treatment of **1** in CH$_2$Cl$_2$ with py gives no reaction, but addition of Me$_3$SiCl leads to formation of the known V$_2$OCl$_4$(py)$_6$ (**3**). The latter is also formed by the reduction of a 1:1 mixture of VOCl$_3$ and VCl$_3$(THF)$_3$ in CH$_2$Cl$_2$/py and by the reaction in CH$_2$Cl$_2$ of VCl$_3$(THF)$_3$ and py with edt^{2-}. Treatment of **1** in MeCN with bpy (2,2′-bipyridine) gives no reaction, but addition of Me$_3$SiCl results in formation and isolation of [V$_2$OCl$_2$-(bpy)$_4$]Cl$_2$ (**4**) identified by spectroscopic comparison with literature data. The reaction of **1** in MeCN with equimolar VCl$_3$(THF)$_3$ and NEt$_4$Cl gives (NEt$_4$)$_3$[V$_3$Cl$_6$(edt)$_3$] (**5**). A more convenient procedure to **5** is the reaction in MeCN of VCl$_3$(THF)$_3$, Na$_2$edt, and NEt$_4$Cl in a 1:1:1 molar ratio. Complex **5**·MeCN crystallizes in triclinic space group $P\bar{1}$ with (at −154 °C) a = 14.918(3) Å, b = 17.142(5) Å, c = 11.276(3) Å, α = 106.78(1)°, β = 95.03(1)°, γ = 106.18(1)°, and Z = 2. The anion contains a near-linear V$_3$ unit with a face-sharing trioctahedral structure: the three edt^{2-} groups provide the six bridging S atoms; two edt^{2-} groups are in a μ-η^2:η^2 mode (as in **1**), but the third is in a μ_3-η^1:η^2:η^1 mode. The V···V separations (>3.1 Å) preclude V−V bonding. Variable-temperature solid-state magnetic susceptibility studies have been performed on complexes **1**, **2**, and **5** in a 1.0 kG field and 5.00−300 K temperature range. For **1**, the effective magnetic moment (μ_{eff}) gradually decreases from 1.09 μ_B at 300 K to 0.26 μ_B at 5.00 K. The data were fit to the Bleaney−Bowers equation, and the fitting parameters were J = −419(11) cm^{-1} and g = 2.05. The singlet−triplet gap is thus 838 cm^{-1}. For **2**, μ_{eff} is essentially temperature-independent, slowly decreasing from 1.90 μ_B at 300 K to 1.86 μ_B at 55 K and then to 1.63 μ_B at 5.00 K. The complex thus is $S = ^1/_2$ with no thermally accessible $S = ^3/_2$ state. The combined data on **1** and **2**, together with the results of EHT calculations, show that **1** and **2** contain a V−V single bond tying up two of the d electrons and that the remaining two d electrons in **1** are antiferromagnetically coupled to give an $S = 0$ ground state and $S = 1$ excited state; for **2**, the one remaining d electron gives an $S = ^1/_2$ state. For **5**, μ_{eff} increases from 5.17 μ_B at 320 K to a maximum of 6.14 μ_B at 30.0 K and then decreases slightly to 6.08 μ_B at 5.00 K. The data were fit to the appropriate theoretical expression to give J = +42.5(6) cm^{-1}, J' = −1.8(5) cm^{-1}, and g = 1.77, where J and J' gauge the interactions between adjacent and terminal V^{III} atoms, respectively. The complex has an $S = 3$ ground state and represents a very rare example of ferromagnetic coupling between V^{III} centers.

Introduction

Our longstanding interest in the syntheses and properties of vanadium/sulfur complexes has been stimulated by a variety of factors, not least of which is the relevance of this area to a number of important industrial processes such as the refining of crude oils by the petroleum industry. Heavy crude oils with large amounts of organic sulfur compounds (thiophenes, thiols, disulfides)[2] also have significant amounts of metallic impurities, chiefly V, Ni, and Fe.[3] The oil-soluble vanadyl species are reduced and sulfided[4−8] and deposited on the catalyst as insoluble vanadium sulfides, which decrease the activity of the catalyst pores.[6,9] The mechanism of formation and deposition of these sulfides (mainly V$_2$S$_3$ and V$_3$S$_4$) is not completely understood, although it has been extensively studied.[3−8] As part of our efforts, we have prepared and studied a variety of V/S complexes,[10] of various nuclearities and oxidation states, to model the V/S intermediates to V$_2$S$_3$/V$_3$S$_4$ that form under the S-rich and reducing conditions of hydrodesulfurization (HDS) and hydrodemetalation (HDM). The mass spectral fragmentation patterns of selected complexes have also been studied as model systems for the high-energy C−S bond cleavage processes occurring in HDS.[10g]

The present report describes an investigation of certain

[⊗] Abstract published in *Advance ACS Abstracts,* October 15, 1996.
(1) Department of Chemistry, Michigan State University.
(2) (a) Orr, W. L. *Oil Sand and Oil Shale Chemistry*; Verlag Chemie: Weinheim, Germany, 1978; p 223. (b) Cyr, T. D.; Payzant, J. D.; Montgomery, D. S.; Strausz, O. P. *Org. Geochem.* **1986**, *9*, 139. (c) Nishioka, M. *Energy Fuels* **1988**, *2*, 214.
(3) Reynolds, J. G.; Biggs, W. R. *Acc. Chem. Res.* **1988**, *21*, 319.
(4) Silbernagel, B. G.; Mohan, R. R.; Singhal, G. H. *ACS Symp. Ser.* **1984**, *248*, 91.
(5) Silbernagel, B. G. *J. Catal.* **1979**, *56*, 315.

(6) Asaoka, S.; Nakata, S.; Shiroto, Y.; Takeuchi, C. *ACS Symp. Ser.* **1987**, *344*, 275.
(7) Rose-Brussin, M.; Moranta, D. *Appl. Catal.* **1984**, *11*, 85.
(8) Mitchell, P. C. H.; Scott, C. E.; Bonnelle, J.-P.; Grimblot, J. G. *J. Chem. Soc., Faraday Trans.* **1985**, *81*, 1047.
(9) Tamm, P. W.; Harnsberger, H. F.; Bridge, A. G. *Ind. Eng. Chem. Process Des. Dev.* **1981**, *20*, 262.

reactivity characteristics of the $[V_2(edt)_4]^{2-}$ (edtH$_2$ = ethane-1,2-dithiol) anion. This species was reported many years ago by three separate groups[11] at nearly the same time, and subjected to crystallographic[11] and electrochemical characterization,[10j,11b] as well as an extended Hückel theory EHT calculation.[12] We recently became interested in the magnetic properties of this species and also its use as a source of other V complexes, including its one-electron-oxidized form and a new trinuclear complex; we herein describe the results of this work.

Experimental Section

Syntheses. All manipulations were carried out under anaerobic conditions employing standard Schlenk and glovebox techniques. MeCN was purified by distillation from CaH$_2$, and Et$_2$O and THF were purified by distillation from Na/benzophenone. Pyridine was purified by a reduced-pressure distillation from CaO. CD$_3$CN was purified by drying over CaH$_2$, followed by vacuum transfer. VCl$_3$, NEt$_4$Cl, NBu$^n_4$-PF$_6$, edtH$_2$, thianthrene, and Me$_3$SiCl were used as purchased and stored under dinitrogen. (NEt$_4$)$_2$[V$_2$(edt)$_4$] **(1)**,[11] VCl$_3$(THF)$_3$,[13] and (C$_{12}$H$_8$S$_2$)-(BF$_4$)[14] (C$_{12}$H$_8$S$_2$ = thianthrene) were prepared by literature methods. Sodium acenaphthylenide (NaACN) was prepared by dissolving Na metal in a THF solution of acenaphthylene.

(NEt$_4$)[V$_2$(edt)$_4$] (2). Method A. A deep blue solution of (C$_{12}$H$_8$S$_2$)-(BF$_4$) (0.106 g, 0.350 mmol) in MeCN (200 mL) was added dropwise to a deep red solution of (NEt$_4$)$_2$[V$_2$(edt)$_4$] (0.256 g, 0.350 mmol) in MeCN (200 mL), and the resulting solution was stirred overnight. The reaction solution slowly became an intense orange-red and a small amount of dark precipitate formed. The mixture was filtered to remove the dark precipitate, and an equal volume of Et$_2$O was added to the filtrate, causing the precipitation of a dark brown solid, which was collected by filtration. This solid was contaminated with NEt$_4$BF$_4$, as evidenced by IR spectroscopy. Purification was accomplished by dissolving the solid in MeCN ($\sim$30 mL) and reprecipitating with THF ($\sim$30 mL), the process being repeated, if necessary, until no BF$_4^-$ stretch could be seen in the IR spectrum. Overall yields were typically low (10−20%), but material was analytically pure. Anal. Calcd (found) for C$_{16}$H$_{36}$NS$_8$V$_2$: C, 32.0 (31.7); H, 6.04 (5.98); N, 2.33 (1.97); V, 17.0 (16.3). Selected IR data (CsI plates, Nujol mull): 1310 (w), 1260 (w), 1181 (w), 1167 (w), 1098 (m), 966 (m, br), 838 (w), 791 (m), 716 (w), 662 (w), 605 (w), 393 (m) cm^{-1}.

Method B. Complex **1** (typically 1 mmol) was dissolved in a 0.10 M solution of NBu$^n_4$PF$_6$ in MeCN ($\sim$30 mL) to give a dark red solution. The potential of the working electrode was set at −0.20 V *vs* Ag/AgCl, and current was allowed to flow through the solution until the excess current flow was essentially zero. The solution color changed from red to orange-red, and the coulombs of charge passed indicated oxidation by 1.09 electrons. Addition of THF produced a dark brown precipitate of **2**, which was purified by reprecipitation from MeCN/THF to remove traces of NBu$^n_4$PF$_6$. The IR spectrum was identical to that of material prepared by method A.

(10) (a) Reynolds, J. G.; Sendlinger, S. C.; Murray, A. M.; Huffman, J. C.; Christou, G. *Inorg. Chem.* **1995**, *34*, 5745. (b) Dean, N. S.; Bartley, S. L.; Streib, W. E.; Lobkovsky, E. B.; Christou, G. *Inorg. Chem.* **1995**, *34*, 1608. (c) York, K. A.; Folting, K.; Christou, G. *J. Chem. Soc., Chem. Commun.* **1993**, 1563. (d) Dean, N. S.; Folting, K.; Lobkovsky, E. B.; Christou, G. *Angew. Chem., Int. Ed. Engl.* **1993**, *32*, 594. (e) Castro, S. L.; Martin, J. D.; Christou, G. *Inorg. Chem.* **1993**, *32*, 2978. (f) Sendlinger, S. C.; Nicholson, J. R.; Lobkovsky, E. B.; Huffman, J. C.; Rehder, D.; Christou, G. *Inorg. Chem.* **1993**, *32*, 204. (g) Heinrich, D. D.; Folting, K.; Huffman, J. C.; Reynolds, J. G.; Christou, G. *Inorg. Chem.* **1991**, *30*, 300. (h) Rambo, J. R.; Eisenstein, O.; Huffman, J. C.; Christou, G. *J. Am. Chem. Soc.* **1989**, *111*, 8027. (i) Christou, G.; Folting, K.; Huffman, J. C.; Heinrich, D. D.; Rambo, J. R.; Money, J. K. *Polyhedron* **1989**, *8*, 1723. (j) Money, J. K.; Huffman, J. C.; Christou, G. *Inorg. Chem.* **1988**, *27*, 507.

(11) (a) Wiggins, R. W.; Huffman, J. C.; Christou, G. *J. Chem. Soc., Chem. Commun.* **1983**, 1313. (b) Dorfman, J. R.; Holm, R. H. *Inorg. Chem.* **1983**, *22*, 3179. (c) Szeymies, D.; Krebs, B.; Henkel, G. *Angew. Chem., Int. Ed. Engl.* **1983**, *22*, 885.

(12) (a) Rao, C. P.; Dorfman, J. R.; Holm, R. H. *Inorg. Chem.* **1986**, *25*, 428. (b) Mukherjee, R. N.; Rao, C. P.; Holm, R. H. *Inorg. Chem.* **1986**, *25*, 2979.

(13) Manzer, L. E. *Inorg. Synth.* **1982**, *21*, 138.

(14) Boduszek, B.; Shine, H. J. *J. Org. Chem.* **1988**, *53*, 5142.

V$_2$OCl$_4$(py)$_6$ (3). Method A. To a stirred solution of VCl$_3$(THF)$_3$ (0.37 g, 1.0 mmol) in CH$_2$Cl$_2$ (25 mL) was added pyridine (0.50 mL, 6.2 mmol), followed by Na$_2$edt (0.14 g, 1.0 mmol); the solution immediately became deep purple, and a light precipitate (NaCl) formed. The reaction mixture was stirred for 4 h and filtered, and the filtrate was layered with Et$_2$O (35 mL). Large purple crystals of **3**·CH$_2$Cl$_2$ slowly formed over several days, and they were found to be suitable for X-ray crystallographic analysis. The bulk material was collected by filtration, washed with Et$_2$O, and dried *in vacuo*. The yield was $\sim$40% (0.15 g). Selected IR data (CsI/Nujol): 1590 (s), 1258 (w), 1209 (m), 1139 (w), 1060 (w), 1030 (w), 758 (w), 749 (m), 741 (w), 713 (m), 683 (m), 622 (w), 611 (w), 430 (w), 372 (w) cm^{-1}. Electronic absorption data in MeCN [λ_{max}, nm (ϵ_M, M^{-1} cm^{-1})]: 290 (sh, 4100), 365 (1800), 538 (4000), 674 (sh, 1300).

Method B. VCl$_3$(THF)$_3$ (0.75 g, 2.0 mmol) was dissolved with stirring in a solution of VOCl$_3$ (190 μL, 2.0 mmol) in CH$_2$Cl$_2$ (20 mL) to give an intensely red solution. To the latter was added NaACN (10 mL of a 0.5 M solution in THF, 5.0 mmol), followed immediately by pyridine (1.0 mL, 12 mmol), producing a deep purple solution and some dark precipitate. The solid was removed by filtration, and Et$_2$O ($\sim$50 mL) was added to the filtrate to give a purple precipitate, which was collected by filtration, washed with Et$_2$O, and dried *in vacuo*; the yield was 30%. The IR and electronic spectra were identical to those for material from method A. Anal. Calcd (found) for C$_{30}$H$_{30}$N$_6$-OCl$_4$V$_2$: C, 49.1 (48.6); H, 4.12 (4.05); N, 11.45 (11.34); Cl, 19.3 (18.4).

Method C. A deep red solution of complex **1** (0.256 g, 0.350 mmol) in MeCN (30 mL) was treated with pyridine (0.40 mL, 4.9 mmol). No color change with time was observed, and the electronic spectrum confirmed that no reaction had occurred. Addition of Me$_3$SiCl (180 μL, 1.4 mmol) caused a rapid color change to deep purple. The electronic spectrum confirmed the formation of V$_2$OCl$_4$(py)$_6$ **(3)**, and solid can be isolated in a manner analogous to method B and in comparable yield.

[V$_2$OCl$_2$(bpy)$_4$]Cl$_2$ (4). A deep red solution of complex **1** (0.256 g, 0.350 mmol) in MeCN (30 mL) was treated with 2,2′-bipyridine (0.109 g, 0.700 mmol). No color change with time was observed, and the electronic spectrum confirmed that no reaction had occurred. Addition of Me$_3$SiCl (180 μL, 1.4 mmol) caused a rapid color change to deep purple. The solution was filtered, the volume of the filtrate reduced by half, and the solution left undisturbed at room temperature for a few days, during which dark purple crystals formed. These were collected by filtration, washed with Et$_2$O, and dried *in vacuo*. Yields were typically >40%. The identity of this product as complex **4** was confirmed by its electronic spectrum, which was identical to that for structurally-characterized material reported in the literature.[15]

(NEt$_4$)$_3$[V$_3$Cl$_6$(edt)$_3$] (5). Method A. VCl$_3$(THF)$_3$ (0.747 g, 2.00 mmol), Na$_2$edt (0.276 g, 2.00 mmol), and NEt$_4$Cl (0.331 g, 2.00 mmol) were slowly dissolved with stirring in MeCN (30 mL). After 2 days, the resulting dark brown solution was filtered to remove NaCl, and Et$_2$O (25 mL) was added to the filtrate. This caused the formation of a small amount of brown precipitate, and this was removed by filtration. The filtrate was left undisturbed at room temperature until block-shaped crystals began to appear (3−5 days), and the flask was then transferred to a freezer for an additional week. The black crystals of **5**·MeCN were collected by filtration, washed with MeCN/Et$_2$O (1:2), and dried *in vacuo*; the yield was 30−40%. Anal. Calcd (found) for C$_{32}$H$_{75}$-N$_4$S$_6$Cl$_6$V$_3$: C, 35.8 (34.8); H, 7.04 (7.04); N, 5.22 (5.48); V, 14.2 (13.9). Selected IR data (CsI, Nujol): 1290 (w), 1175 (w), 1166 (w), 1020 (s), 780 (w), 715 (w), 522 (w), 512 (w), 345 (s), 330 (s), 300 (s, br), 280 (s), 268 (s) cm^{-1}.

Method B. Complex **1** (0.256 g, 0.350 mmol), VCl$_3$(THF)$_3$ (0.262 g, 0.700 mmol), and NEt$_4$Cl (0.116 g, 0.700 mmol) were dissolved with stirring in MeCN (20 mL). The initial red color of the solution slowly changed to dark brown. The solution was filtered to remove a small amount of dark precipitate, and Et$_2$O (15 mL) was added to the filtrate to slowly give a brown, microcrystalline precipitate in $\sim$30% yield. Storage of the flask in the freezer increased the yield of product to $\sim$40%. The material was spectroscopically identical to material from method A.

(15) Brand, S. G.; Edelstein, N.; Hawkins, C. J.; Shalimoff, G.; Snow, M. R.; Tiekink, E. R. T. *Inorg. Chem.* **1990**, *29*, 434.

Table 1. Crystallographic Data for $(NEt_4)_3[V_3Cl_6(edt)_3] \cdot MeCN$ (**5·MeCN**)

formula[a]	$C_{32}H_{75}N_4S_6Cl_6V_3$	Z	2
fw	1073.86	T, °C	−154
space group	$P\bar{1}$	λ, Å[b]	0.710 69
a, Å	14.918(3)	ρ_{calc}, g/cm^3	1.368
b, Å	17.142(5)	μ, cm^{-1}	10.782
c, Å	11.276(3)	no. of unique data	4718
α, deg	106.78(1)	no. of obsd data	1962
β, deg	95.03(1)	$(F > 3\sigma(F))$	
γ, deg	106.18(1)	$R\ (R_w)$,[c] %	8.87 (8.55)
V, Å^3	2606.8		

[a] Including solvate molecule. [b] Mo Kα; graphite monochromator. [c] $R = \sum ||F_o| - |F_c||/\sum |F_o|$. $R_w = [\sum w(|F_o| - |F_c|)^2/\sum w|F_o|^2]^{1/2}$ where $w = 1/\sigma^2(|F_o|)$.

X-ray Crystallography and Structure Solution. Data were collected for complex **5·MeCN** on a Picker four-circle diffractometer; details of the diffractometry, low-temperature facilities, and computational procedures employed by the Molecular Structure Center are available elsewhere.[16] A suitable, well-formed crystal was selected from the bulk sample using inert-atmosphere handling techniques and transferred to a goniostat where it was cooled for characterization and data collection. A systematic search of a limited hemisphere of reciprocal space yielded a set of reflections with no symmetry or systematic absences, indicating a triclinic space group, $P1$ or $P\bar{1}$. The choice of the centrosymmetric space group $P\bar{1}$ was confirmed by the subsequent successful solution and refinement of the structure. Approximately midway through the data collection, the crystal split, but data collection was continued with a remaining fragment, which still diffracted well, and the intensities of the latter data set were adjusted by multiplying by an appropriate scale factor determined from reflections measured before and after crystal cleavage. Following the usual data reduction, a unique set of 4718 reflections was obtained, of which only 1962 were considered observed by the criterion $F > 3\sigma(F)$. The R for averaging of redundant data was quite high at 0.318. No absorption correction was carried out, and the plot of four standard reflections showed no systematic trends. The structure was solved by direct methods (MULTAN), followed by successive difference Fourier maps phased with the atoms already located. All non-hydrogen atoms were readily located and refined with anisotropic thermal parameters. The full-matrix least-squares refinement on F was completed with hydrogen atoms included in fixed, idealized positions. The final difference map was essentially featureless; final $R\ (R_w)$ values are included in Table 1.

Physical Measurements. Infrared spectra were recorded as Nujol mulls on CsI plates using Perkin-Elmer 283 and Nicolet 510P FTIR spectrophotometers. Electronic spectra were recorded in solution in 0.02 and 0.05 cm quartz cells using a Hewlett-Packard 8452A spectrophotometer. Variable-temperature magnetic susceptibility measurements were obtained at Michigan State University with a Quantum Design MPMS SQUID susceptometer operating with a 1.0 kG (1 T) applied magnetic field. The experimental magnetic susceptibilities were corrected for the diamagnetic response using Pascal's constants. Cyclic voltammograms were recorded on BAS CV-27 and CV-50 W instruments using a standard three-electrode assembly (Ag wire working, Pt wire auxiliary, Ag/AgCl reference) and 0.1 M NBu$^n_4$PF$_6$ as supporting electrolyte. The scan rate was 100 mV/s and no iR compensation was employed. Controlled-potential electrolysis was performed using a similar setup, but with a larger surface area Pt mesh working electrode and the Pt wire auxiliary electrode isolated by a fritted disk from the solution of the complex. EPR spectra were recorded on a Bruker ESP 300D spectrometer operating at ~9.4 GHz (X-band); accurate magnetic field values at various spectral positions were obtained with an external gaussmeter. NMR spectra were recorded on a Varian XL300 spectrometer. Evan's method determinations of magnetic susceptibility were performed using 5 mm tubes with coaxial inserts. Magnetic susceptibilities were determined using the standard equation. Diamagnetic correction factors were estimated using Pascal's constants.

(16) Chisholm, M. H.; Folting, K.; Huffman, J. C.; Kirkpatrick, C. C. *Inorg. Chem.* **1984**, *23*, 1021.
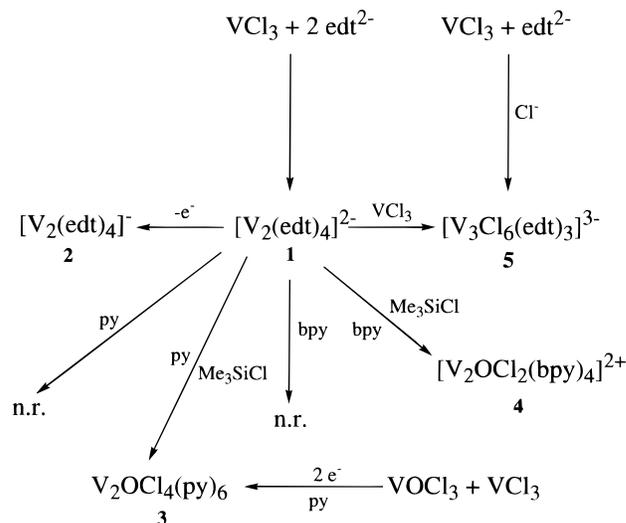
Figure 1. Summary of the transformations described in the text, and the compound numbering scheme (for salts, only one ion is shown).

Results

Reactivity Characteristics of $[V_2(edt)_4]^{2-}$. For convenience, a summary of the transformations to be described is presented in Figure 1. For solubility reasons, the NEt$_4^+$ salt (i.e., complex **1**) was employed.

Oxidation Reactions. The $[V_2(edt)_4]^{2-}$ anion has previously been reported[10j,11b] to display two oxidation processes when studied by cyclic voltammetry, a one-electron reversible oxidation and a second, irreversible one-electron oxidation. In the present work, these processes were measured in MeCN solution at −0.48 V and −0.01 V (E_p *vs* Ag/AgCl); the first oxidation feature has $i_f/i_r \approx 1$ (f = forward, r = reverse) throughout the scan rate (v) range 50−500 mV/s. Plots of i *vs* $v^{1/2}$ for both i_f and i_r give a linear dependence in this scan rate range, indicating a diffusion-controlled process. The one-electron nature of this oxidation was previously demonstrated by coulometry ($n = 1.00 \pm 0.05$).[10j]

Isolation of the $[V_2(edt)_4]^-$ monoanion was sought by both chemical and electrochemical oxidation, and both methods proved successful. Controlled-potential electrolysis of large quantities (typically ~1 mmol ≈ 0.75 g) at −0.20 V *vs* Ag/AgCl in MeCN containing NBu$^n_4$PF$_6$ gave an orange-red color characteristic of the monoanion, which could be precipitated by addition of THF in which the supporting electrolyte is soluble. Precipitates were nevertheless invariably contaminated with NBu$^n_4$PF$_6$, necessitating reprecipitation from MeCN/THF until pure, lowering yields to ~20%.

A more convenient procedure is chemical oxidation; initial attempts employing ferrocenium salts or I$_2$ had given impure products, probably due to degradative attack on the anion, but a superior procedure was developed using the radical cation of thianthrene as the oxidant to ensure outer-sphere electron

thianthrene (Thn)
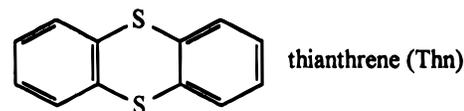
transfer. This radical can be readily prepared[14] as the BF$_4^-$ salt and has a potential of +0.30 V. This represents sufficient oxidizing strength to accomplish the two-electron oxidation of **1**, and initial experiments were unfortunately extensively plagued by such complications. Employment of dilute solutions and slow, dropwise addition of an equimolar thianthrenium solution gave essentially clean, one-electron oxidation, however, and

analytically pure preparations of $(NEt_4)[V_2(edt)_4]$ (**2**) could be obtained after recrystallizations to remove contaminating NEt_4-BF_4 (eq 1). Products from the two routes to complex **2** display

$$(NEt)_2[V_2(edt)_4] + (Thn)BF_4 \rightarrow$$
$$(NEt_4)[V_2(edt)_4] + Thn + NEt_4BF_4 \quad (1)$$
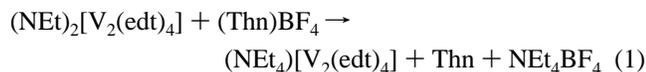
identical IR spectra. Complex **2** is stable in the solid state and in solution under an inert atmosphere. Unfortunately, numerous attempts to obtain single crystals of **2** suitable for crystallography proved unsuccessful.

Reactions with Lewis Bases. Treatment of complex **1** in MeCN solution with an excess of py, bpy, or PMe_2Ph gave no reaction, as confirmed by electronic spectral monitoring of the dark red solutions with time. The absence of even adduct formation attests to the stability and electron-rich nature of this anion. Addition of 4 equiv of Me_3SiCl to the py reaction solution triggers a reaction and the formation of a deep purple solution assignable to known $V_2OCl_4(py)_6$ (**3**) (method C) on the basis of electronic spectral comparison with published data.[17] The loss of all edt^{2-} groups and the presence of an oxide bridge suggested incorporation of a H_2O molecule with the edt^{2-} groups acting as H^+ acceptors, $edtH_2$ ($pK_{a_1} = 9.05$, $pK_{a_2} = 10.56$) being a much weaker acid than pyridinium ($pK_a = 5.25$), as summarized in eq 2. The ability of edt^{2-} to act as a Brønsted base

$$[V_2(edt)_4]^{2-} + 4Me_3SiCl + H_2O \xrightarrow{+6py}$$
$$V_2OCl_4(py)_6 + 2edtH^- + 2(Me_3Si)_2edt \quad (2)$$
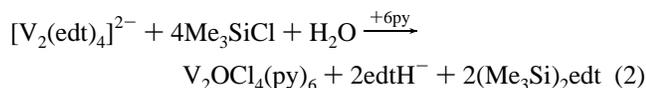
and facilitate oxide bridge formation was supported by an alternative procedure (method B) developed for **3** involving addition of equimolar Na_2edt to a $VCl_3(THF)_3$/py reaction mixture in CH_2Cl_2, giving a deep purple solution from which was subsequently isolated $3\cdot CH_2Cl_2$ as large purple crystals (eq 3). A crystal structure determination was carried out on $3\cdot$

$$2VCl_3 + 6py + 2Na_2edt + H_2O \rightarrow$$
$$V_2OCl_4(py)_6 + 2NaHedt + 2NaCl \quad (3)$$
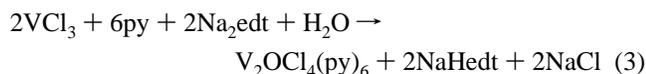
CH_2Cl_2 to confirm the identity of material from this route; brief details were previously published,[10i] and the full results are provided in the Supporting Information.

A third procedure to **3** (Method B) was devised involving acenaphthylenide reduction of an equimolar mixture of $VOCl_3$ and $VCl_3(THF)_3$ in CH_2Cl_2, followed by addition of py to generate a deep purple solution of **3** (eq 4). This preparation is

$$VOCl_3 + VCl_3 + 2e^- + 6py \rightarrow V_2OCl_4(py)_6 + 2Cl^- \quad (4)$$
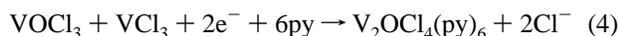
somewhat related to one of the two previously reported routes to **3**,[17] which involves a V^{II} reagent, *viz.* the reaction between $VCl_2(py)_4$ and $VOCl_2(py)_2$ or PhIO.

Addition of Me_3SiCl to the deep red mixture of **1** and bpy triggered reaction and formation of a deep purple solution from which was isolated $[V_2OCl_2(bpy)_4]Cl_2$ (**4**), identified by spectral comparison with published data.[15] All edt^{2-} groups are again lost, and an equation analogous to eq 2 can be presented to summarize the reaction (eq 5).

$$[V_2(edt)_4]^{2-} + 4bpy + 4Me_3SiCl + H_2O \rightarrow$$
$$[V_2OCl_2(bpy)_4]Cl_2 + 2(Me_3Si)_2edt + 2edtH^- \quad (5)$$

(17) Zhang, Y.; Holm, R. H. *Inorg. Chem.* **1990**, *29*, 911.
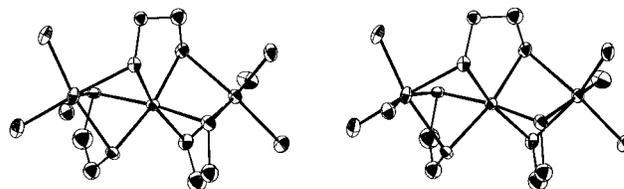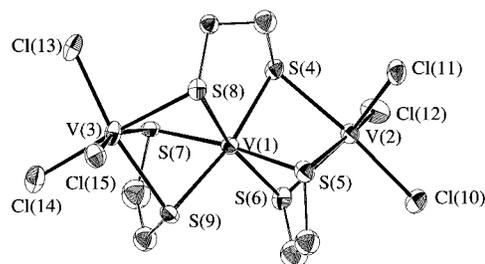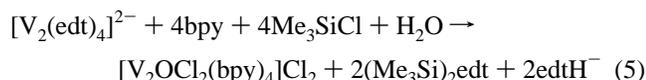
Figure 2. ORTEP representation and stereoview at the 50% probability level of the anion of **5** from a viewpoint approximately perpendicular to the virtual C_2 axis.

Reaction with $VCl_3(thf)_3$. Complex **1** in MeCN reacted rapidly with $MCl_3(THF)_3$ (M = V, Mo) or $FeCl_3$. For the Mo and Fe reactions, the reaction mixtures deposited microcrystalline solids whose very low solubility has hampered characterization. For M = V, however, a dark brown solution was generated from which could be isolated $(NEt_4)_3[V_3Cl_6(edt)_3]$ (**5**); after product characterization, the requirement was recognized for extra NEt_4^+ and Cl^- for stoichiometric reaction, and subsequent preparations (method B) employed added NEt_4Cl, as summarized in eq 6. The product has a tendency to oil out of the

$$3(NEt_4)_2[V_2(edt)_4] + 6VCl_3 + 6NEt_4Cl \rightarrow$$
$$4(NEt_4)_3[V_3Cl_6(edt)_3] \quad (6)$$
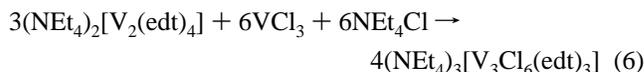
mother liquor on addition of Et_2O, and crystallization must be initiated at room temperature before placing in the freezer. With the identity of **5** established, a direct synthetic procedure (method A) was developed employing a $VCl_3/edt^{2-}/Cl^-$ reaction ratio of 1:1:1, corresponding to eq 7.

$$3VCl_3 + 3Na_2edt + 3NEt_4Cl \rightarrow$$
$$(NEt_4)_3[V_3Cl_6(edt)_3] + 6NaCl \quad (7)$$
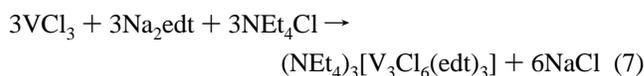
Description of the Structure. An ORTEP representation of the anion of **5** is shown in Figure 2; fractional coordinates and selected interatomic distances and angles are collected in Tables 2 and 3. The anion of **5** consists of a nearly linear arrangement of three V^{III} atoms ($V(3)-V(1)-V(2) = 167.3°$) with three monoatomic S bridges between each V_2 pair. The structure is thus three face-sharing octahedra. The central $V(1)$ atom has a VS_6 coordination environment, and the structure could be described as an adduct between a $[V(edt)_3]^{3-}$ trischelate and two Lewis acidic VCl_3 units. Two of the edt^{2-} groups are in the same $\mu-\eta^2,\eta^2$ mode seen in $[V_2(edt)_4]^{2-}$ (below) while the other is in a rarer $\mu_3-\eta^1,\eta^2,\eta^1$ mode. The V–S distances to central $V(1)$ ($2.377(10)-2.430(10)$ Å) are similar to those to $V(2)$ and $V(3)$ ($2.466(9)-2.506(10)$ Å), and the terminal V–Cl distances ($2.321(10)-2.400(11)$ Å) are similar to those in $[V_2Cl_7(THF)_2]^-$ ($2.286(2)-2.328(2)$ Å).[18] The trischelate description for $V(1)$ and the three five-membered VS_2C_2 rings causes the geometry at $V(1)$ to be significantly more distorted from octahedral than those at $V(2)$ and $V(3)$. The V···V

(18) Rambo, J. R.; Bartley, S. L.; Streib, W. E.; Christou, G. *J. Chem. Soc., Dalton Trans.* **1994**, 1813.

Table 2. Selected Fractional Coordinates ($\times 10^4$) and Equivalent[a] or Actual Isotropic Thermal Parameters ($\text{Å}^2 \times 10$)[a] for $(NEt_4)_3[V_3Cl_6(edt)_3]\cdot MeCN$ (**5·MeCN**)

atom	x	y	z	B_{iso}, B_{eq}
V(1)	9736(3)	2380(3)	3390(6)	16
V(2)	7569(3)	1518(4)	3230(6)	20
V(3)	11923(3)	2826(4)	3312(6)	21
S(4)	8625(5)	1316(6)	1632(8)	20
S(5)	8510(5)	3062(6)	3677(9)	24
S(6)	8962(5)	1823(5)	4900(9)	24
S(7)	10639(5)	3071(5)	2086(8)	19
S(8)	10696(4)	1461(5)	3218(8)	17
S(9)	11068(5)	3495(5)	4897(9)	24
Cl(10)	6647(5)	1857(6)	4799(9)	30
Cl(11)	7106(5)	57(5)	3000(9)	27
Cl(12)	6489(5)	1587(6)	1683(9)	35
Cl(13)	12447(5)	2035(6)	1595(8)	24
Cl(14)	13022(5)	4179(6)	3425(9)	31
Cl(15)	12903(5)	2680(6)	4925(8)	27
C(16)	10180(17)	728(20)	1628(29)	18(6)
C(17)	9097(19)	446(21)	1471(32)	25(6)
C(18)	8739(22)	3414(25)	5379(38)	39(7)
C(19)	8910(20)	2791(23)	5995(35)	31(7)
C(20)	10798(23)	4183(26)	2907(40)	43(8)
C(21)	11016(20)	4399(23)	4338(35)	30(7)

[a] $B_{eq} = (4/3)\Sigma\Sigma B_{ij}a_i a_j$.

Table 3. Selected Bond Distances (Å) and Angles (deg) for $(NEt_4)_3[V_3Cl_6(edt)_3]\cdot MeCN$

V(1)−V(2)	3.121(8)	V(2)−Cl(12)	2.321(10)
V(1)−V(3)	3.147(8)	V(2)−S(4)	2.506(9)
V(1)−S(4)	2.377(10)	V(2)−S(5)	2.503(11)
V(1)−S(5)	2.428(8)	V(2)−S(6)	2.505(9)
V(1)−S(6)	2.411(11)	V(3)−Cl(13)	2.353(10)
V(1)−S(7)	2.417(10)	V(3)−Cl(14)	2.400(11)
V(1)−S(8)	2.387(8)	V(3)−Cl(15)	2.347(10)
V(1)−S(9)	2.430(10)	V(3)−S(7)	2.466(9)
V(2)−Cl(10)	2.376(9)	V(3)−S(8)	2.505(10)
V(2)−Cl(11)	2.334(10)	V(3)−S(9)	2.485(9)

S(4)−V(1)−S(5)	85.6(3)	Cl(12)−V(2)−S(6)	165.2(4)
S(4)−V(1)−S(6)	93.5(3)	S(4)−V(2)−S(5)	81.4(3)
S(4)−V(1)−S(7)	93.2(3)	S(4)−V(2)−S(6)	88.2(3)
S(4)−V(1)−S(8)	89.0(3)	S(5)−V(2)−S(6)	74.5(3)
S(4)−V(1)−S(9)	169.1(4)	Cl(13)−V(3)−Cl(14)	93.9(3)
S(5)−V(1)−S(6)	77.6(3)	Cl(13)−V(3)−Cl(15)	97.7(3)
S(5)−V(1)−S(7)	102.6(3)	Cl(13)−V(3)−S(7)	97.4(3)
S(5)−V(1)−S(8)	167.2(4)	Cl(13)−V(3)−S(8)	88.9(3)
S(5)−V(1)−S(9)	100.3(3)	Cl(13)−V(3)−S(9)	169.3(3)
S(6)−V(1)−S(7)	173.3(4)	Cl(14)−V(3)−Cl(15)	92.7(3)
S(6)−V(1)−S(8)	91.2(3)	Cl(14)−V(3)−S(7)	91.6(3)
S(6)−V(1)−S(9)	96.6(4)	Cl(14)−V(3)−S(8)	176.2(3)
S(7)−V(1)−S(8)	89.3(3)	Cl(14)−V(3)−S(9)	93.7(3)
S(7)−V(1)−S(9)	76.7(3)	Cl(15)−V(3)−S(7)	164.0(3)
S(8)−V(1)−S(9)	86.9(3)	Cl(15)−V(3)−S(8)	89.4(3)
Cl(10)−V(2)−Cl(11)	94.2(3)	Cl(15)−V(3)−S(9)	89.6(4)
Cl(10)−V(2)−Cl(12)	92.3(3)	S(7)−V(3)−S(8)	85.6(3)
Cl(10)−V(2)−S(4)	174.3(4)	S(7)−V(3)−S(9)	74.8(3)
Cl(10)−V(2)−S(5)	92.9(3)	S(8)−V(3)−S(9)	83.2(3)
Cl(10)−V(2)−S(6)	90.4(3)	V(1)−S(4)−V(2)	79.4(3)
Cl(11)−V(2)−Cl(12)	103.1(4)	V(1)−S(5)−V(2)	78.5(3)
Cl(11)−V(2)−S(4)	91.3(3)	V(1)−S(6)−V(2)	78.8(3)
Cl(11)−V(2)−S(5)	164.0(3)	V(1)−S(7)−V(3)	80.4(3)
Cl(11)−V(2)−S(6)	91.2(3)	V(1)−S(8)−V(3)	80.2(3)
Cl(12)−V(2)−S(4)	87.8(4)	V(1)−S(9)−V(3)	79.8(3)
Cl(12)−V(2)−S(5)	90.8(4)		

separations (3.121(8), 3.147(8) Å) are much longer than that in the parent $[V_2(edt)_4]^{2-}$ anion (~2.60 Å), consistent with the triply-bridged *vs* quadruply-bridged nature of **5** *vs* **1** and the absence of V−V bonding in the former (*vide infra*).

Electronic Structure of $[V_2(edt)_4]^{2-}$. An EHT calculation on $[V_2(edt)_4]^{2-}$ was reported by Rao *et al.*,[12] and the important points are the following: With the z axis defined as the V−V vector, the lowest, occupied d-type frontier orbital is formed

anion of **1**
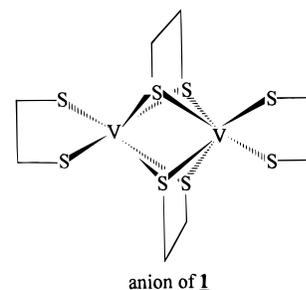
by d_{z^2} overlap and represents a V−V σ-bonding orbital. Approximately 0.6−0.7 eV (4800−5600 cm^{-1}) above this lie the HOMO and LUMO consisting of closely-spaced (0.17 eV) δ^* and δ orbitals, respectively, formed by overlap of vanadium $d_{x^2-y^2}$ orbitals. These orbitals also have significant sulfur p character, which is responsible for the abnormal ordering of the δ and δ^* orbitals. There is then a gap of ~1.2 eV (9700 cm^{-1}) to the SLUMO. This picture of $[V_2(edt)_4]^{2-}$ is very similar to that more recently found for $[V_2O(SPh)_4(Me_2bpy)_2]$ (**6**; Me_2bpy = 4,4′-dimethyl-2,2′-bipyridine),[10b] where a σ-bonding (d_{z^2}/d_{z^2}) orbital was well-separated (0.54 eV) from a HOMO/LUMO pair of δ/δ^* character, the latter being closely spaced (~0.02 eV, ~150 cm^{-1}). The SLUMO was 0.31 eV (2500 cm^{-1}) above the δ^* orbital. For **6**, the overlap populations of the δ and δ^* orbitals are very small (<0.04 electron), and the same situation is present in **1**, such that the closely-spaced HOMO and LUMO can reasonably be described as essentially localized on single metals and consequently V−V nonbonding in nature.

Both **1** and **6** therefore appear to have very similar electronic structures with $S = 0$ ground states of configurations $\sigma^2\delta^{*2}$ for **1** and $\sigma^2\delta^2$ for **6**, with a net V−V single bond. With a small HOMO/LUMO gap, the $\sigma^2\delta^*\delta$ (**1**) and $\sigma^2\delta\delta^*$ (**6**) excited states ($S = 1$) should be low-lying and possibly thermally populated at room temperature, leading to the complexes being paramagnetic: this was indeed found for **6**. For **1**, a μ_{eff}/V_2 value of 0.88 ± 0.10 μ_B at 297 K has been reported[12b] and suggests a similar population of the triplet excited state. Inasmuch as the one-electron energies resulting from an EHT calculation are not an accurate assessment of the true energies in a multielectron system, an accurate determination of the singlet−triplet energy gap in **1** requires variable-temperature magnetic susceptibility data to probe the population of the triplet excited state as a function of temperature.

Magnetic Susceptibility Studies. Variable-temperature, solid-state magnetic susceptibility data were collected on powdered samples of complexes **1**, **2**, and **5** in a 1.0 kG applied magnetic field and in the temperature range 5.0−300 K.

For $(NEt_4)_2[V_2(edt)_4]$ (**1**), the effective magnetic moment (μ_{eff}) per V_2 decreases from 1.09 μ_B at 300 K to 0.26 μ_B at 5.00 K (Figure 3). The 300 K value corresponds to 0.77 μ_B per V, much less than the spin-only values for one or two unpaired electrons of 1.73 and 2.83 μ_B, respectively. The data were fit to the Bleaney−Bowers equation (eq 8) based on the spin-

$$\chi_M = \frac{2Ng^2\mu_B^2}{kT}\left[\frac{1}{3+\exp(2x)}\right](1-\rho) + \frac{2\rho Ng^2\mu_B^2}{3kT} + \text{TIP} \quad (8)$$

Hamiltonian $\hat{H} = -2J\hat{S}_1\hat{S}_2$, where $x = -J/kT$, N is Avogadro's number, ρ is the mole fraction of paramagnetic impurity (assumed to be mononuclear V^{III} and giving the second term in eq 8), TIP is the temperature-independent paramagnetism, and the other symbols have their usual meaning. The use of eq 8 assumes that complex **1** behaves as a d^1/d^1 system because two

Figure 3. Plots of molar magnetic susceptibility (χ_M) *vs* temperature (●) and effective magnetic moment (μ_{eff}) *vs* temperature (♦) for complex **1**. The solid lines are fits of the data to eq 8; see the text for fitting parameters.

Figure 4. Plots of molar magnetic susceptibility (χ_M) *vs* temperature (●) and effective magnetic moment (μ_{eff}) *vs* temperature (♦) for complex **2**. The data points are joined together as a visual aid.

d electrons are tied up in a relatively low-lying bonding orbital (*vide supra*).

Fitting of the data to eq 8 gave a satisfactory fit with $J = -419$ cm^{-1}, $g = 2.05$, and $\rho = 0.0073$, with TIP held constant at 300×10^{-6} cm^3 mol^{-1}; this fit is shown as a solid line in Figure 3. Also shown is a fit to the data plotted as μ_{eff} *vs* T. The singlet–triplet gap is thus $|2J| = 838$ cm^{-1} or approximately 0.10 eV. This may be compared with the 0.17 eV (1370 cm^{-1}) HOMO–LUMO gap in the EHT calculation; as stated earlier, the one-electron energies given by the MO calculation are not an accurate estimate of the true singlet–triplet gap in a multielectron system, so the observed degree of similarity is quite satisfying. A value of 838 cm^{-1} results in ~5% of the [V$_2$(edt)$_4$]$^{2-}$ anions being in the $S = 1$ excited state at room temperature (~300 K).

For (NEt$_4$)[V$_2$(edt)$_4$] (**2**), μ_{eff}/V$_2$ is essentially temperature-independent at higher temperatures, slowly decreasing from 1.90 μ_B at 300 K to 1.86 μ_B at 55 K and then decreasing more rapidly to 1.63 μ_B at 5.00 K (Figure 4). These data are consistent with an $S = {}^1/_2$ spin system with no thermally accessible excited states in the 5.0–300 K region. The slight decrease at low temperatures is likely due to weak *inter*molecular interactions between [V$_2$(edt)$_4$]$^-$ ions that are antiferromagnetic.

For (NEt$_4$)$_3$[V$_3$Cl$_6$(edt)$_3$]·MeCN (**5·MeCN**), μ_{eff}/V$_3$ gradually increases from 5.17 μ_B at 320 K to a maximum of 6.14 μ_B at 30.0 K and then decreases slightly to 6.08 μ_B at 5.00 K (Figure 5). These data suggest the presence of (at least some) ferromagnetic exchange interactions in the anion of **5**, and the

Figure 5. Plots of molar magnetic susceptibility (χ_M) *vs* temperature (♦) and effective magnetic moment (μ_{eff}) *vs* temperature (●) for complex **5**. The solid lines are fits of the data to the appropriate theoretical equation; see the text for fitting parameters.

low-temperature values may be compared with the spin-only ($g = 2$) value of 6.93 μ_B for an $S = 3$ spin system.

The Heisenberg spin Hamiltonian that describes the possible pairwise interactions for a linear trinuclear species

$$V(3)\overset{J}{\text{—}}V(1)\overset{J}{\text{—}}V(2)$$
$$\underset{J'}{\underbrace{\phantom{V(3)\text{—}V(1)\text{—}V(2)}}}$$

is given by eq 9, where $J = J_{13} = J_{12}$ and $J' = J_{23}$; S_i is the spin

$$\hat{H} = -2J(\hat{S}_1\hat{S}_3 + \hat{S}_1\hat{S}_2) - 2J'(\hat{S}_2\hat{S}_3) \qquad (9)$$

operator for metal V(i). Using the Kambe vector coupling method[19] and the coupling scheme $\hat{S}_A = \hat{S}_2 + \hat{S}_3$ and $\hat{S}_T = \hat{S}_A + \hat{S}_1$, eq 9 can be expressed in the equivalent form of eq 10,

$$\hat{H} = -J(\hat{S}_T{}^2 - \hat{S}_A{}^2 - \hat{S}_1{}^2) - J'(\hat{S}_A{}^2 - \hat{S}_2{}^2 - \hat{S}_3{}^2) \quad (10)$$

where S_T are the spin states of the entire V$_3$ unit. The energies (E) of the spin states (S_T) are given by eq 11, where constant

$$E = -J[S_T(S_T + 1) - S_A(S_A + 1)] - J'[S_A(S_A + 1)] \quad (11)$$

terms have been ignored. For complex **5**, $S_1 = S_2 = S_3 = 1$, and the overall degeneracy of this spin system is 27, made up of seven individual spin states with S_T values ranging from 0 to 3.

A theoretical χ_M *vs* T expression was derived using eq 11 and the Van Vleck equation, and this was used to fit the data for complex **5**: a satisfactory fit was obtained with $J = 42.5(6)$ cm^{-1}, $J' = -1.8(5)$ cm^{-1}, and $g = 1.769(1)$, with the TIP held constant at 800×10^{-6} cm^3 mol^{-1}. The fit is shown as a solid line in Figure 5. The ground state is $S_T = 3$ arising from a $S_A = 2$ term, i.e., (3, 2) in the format (S_T, S_A). The excited states are (2,1), (1,0), (1,1), (2,2), (0,1), and (1,2) at energies of 77.8, 159.2, 247.8, 255, 332.8, and 425 cm^{-1}, respectively, above the ground state. The ground state is thus fairly well isolated from the first excited state. Note that the fit (solid line in Figure 5) does not reproduce the slight decrease in μ_{eff} at temperatures ≤15 K; the latter is likely due to a combination of zero-field splitting of the $S = 3$ ground state, Zeeman effects, and weak *inter*molecular exchange interactions that are antiferromagnetic. Data at ≤7 K were omitted from the fit.

(19) Kambe, K. *J. Phys. Soc. Jpn.* **1950**, *48*, 15.

Figure 6. X-band EPR spectra of complex **2** in EtCN at the indicated temperatures. See the text for *g* and *A* values.

In view of our previous experience that both global and local minima may be encountered in fits of susceptibility data,[20,21d] relative (root mean square) error surfaces were generated for **1** and **5**. Complex **1** is a single-*J*-value system, and the relative error surface as a function of *J* and *g* shows only a single minimum. For complex **5**, the relative error surface as a function of *J*, *J′*, and *g* gave two minima: $J = 42.5(6)$ cm^{-1}, $J′ = -1.8(5)$ cm^{-1}, and $g = 1.769(1)$, as given earlier, and $J = 13.9(2)$ cm^{-1}, $J′ = 55.7(9)$ cm^{-1}, and $g = 1.768(1)$. The two fits have comparable rms error values, with the latter fit being very slightly better, in fact, but it is nevertheless discounted as giving a chemically unreasonable conclusion that the *J′* (V(2)···V(3)) coupling would be much stronger than *J* (V(1)···V(2) and V(1)···V(3)).

EPR Spectroscopy. Complexes **1** and **5** are EPR-inactive, but the $S = ^1/_2$ nature of **2** suggests it should display an EPR signal. The room-temperature X-band spectrum of **2** in MeCN shows a signal at $g \sim 2$ with an approximate eight-line pattern but with some additional splitting of the resonances. While this is consistent with an $S = ^1/_2$ system, the spectrum is neither the simple eight-line signal expected for an unpaired electron coupled to a single V nucleus (^{51}V, $I = ^7/_2$, ~100%) nor the 15-line signal expected for an electron that is fully delocalized over two equivalent V nuclei or rapidly detrapping at a rate that is fast on the EPR time scale. On cooling of the sample to 260 K in EtCN solution, the spectrum becomes a clear, albeit broadened, eight-line signal (Figure 6) with $g_{iso} = 1.986$ and $A_{iso} = 77$ G, typical of a mononuclear V^{IV} species, for example, and suggesting an essentially trapped electron on the EPR time scale. Further temperature reduction forms a frozen solution and at 77 K gives a typical V^{IV} anisotropic (axial) spectrum, with $g_{\|} = 1.968$ ($A_{\|} = 145$ G) and $g_{\perp} = 1.995$ ($A_{\perp} = 43$ G).

The increased broadening over that normally observed for mononuclear V^{IV} species may be due to smaller, unresolved hyperfine coupling with the second V nucleus. The EPR data thus suggest a Robin–Day class II[22] mixed-valence system showing relatively slow detrapping (hopping) between the two V atoms. On heating of the sample to 320 and 380 K, the spectrum becomes more complicated with ~13 lines observable, but instrumental limitations precluded the possibility of reaching a temperature where an isotropic 15-line signal might be observed.

Related behavior has been previously observed: for example, the complexes $[P_2W_{16}V_2O_{62}]^{9-}$ and $[P_2W_{15}V_3O_{62}]^{10-}$ contain V^{IV},V^V and V^{IV},2V^V, respectively, and at 353 °C in aqueous solution exhibit 15-line and 22-line EPR signals,[23] respectively, consistent with rapid detrapping of the unpaired electrons between the V atoms. At 77 K, however, both complexes show the same broadened, anisotropic signals typical of mononuclear V^{IV}, indicating that the detrapping rate is now slow on the EPR time scale. More recently, the V^{IV},V^V species $[V_2O_3L_2]^-$ (L = tridentate, diolate ligands)[24] were also been found to give isotropic 15-line signals in fluid solution at 300 K but "mono-nuclear-like" anisotropic signals at 77 K ($g_{\|} = 1.950-1.960$, $A_{\|} \approx 174$ G, $g_{\perp} = 1.979-1.983$, $A_{\perp} = 61-64$ G).

Discussion

The present work demonstrates that the $[V_2(edt)_4]^{2-}$ anion of **1** is a useful steppingstone to other V species. Its one-electron oxidation by an outer-sphere oxidizing agent (thianthrenium or an electrode at an appropriate potential) leads to the mixed-valence $[V_2(edt)_4]^-$ anion of **2**. Numerous attempts to obtain **2** in a form suitable for crystallographic studies have unfortunately proven unsuccessful, but there is no doubt from the combined elemental analysis and magnetochemical and EPR spectral data that **2** is correctly formulated; **2** also gives the same cyclic voltammetry response as **1**, except that the feature at −0.48 V is now a reduction.

The treatment of **1** with an excess of py or bpy gives no reaction and attests to the stability of this anion, but addition of Me$_3$SiCl triggers reaction, no doubt by removal of terminal edt^{2-} groups as the silyl esters, to give **3**[10i,17] and **4**,[15] both of which have been previously reported. Both complexes possess [VOV]$^{4+}$ units, and the present preparations appear to suggest that edt^{2-} groups are acting as H$^+$ acceptors, facilitating O^{2-} formation from H$_2$O; edt^{2-} is a good Brønsted base, as indicated by the pK_a values for edtH$_2$ at 25 °C (pK_{a_1} = 9.05, pK_{a_2} = 10.56), compared with py (pyH$^+$: pK_a = 5.25).

In contrast to py and bpy reactions, the reaction with VCl$_3$(THF)$_3$ proceeds rapidly and gives the $[V_3Cl_6(edt)_3]^{3-}$ anion of **5**, the reaction presumably involving electrophilic attack by Lewis acidic VCl$_3$ at the terminal edt^{2-} groups. The resulting near-linear V$^{III}_3$ structure of **5** is unusual: most known trinuclear V complexes at the ~III oxidation state have a triangular structure, often with a central μ_3-oxide[21] or μ_3-sulfide[10j,25] ion, and only a few linear V$_3$ species are known, including [V$_3$(O$_2$CR)$_6$(tmeda)$_2$][26a] (3V^{II}), [V$_3$(mp)$_6$]$^-$ [26b] (V^{III},2V^{IV}; mpH$_2$ =

(20) McCusker, J. K.; Jang, H. G.; Wang, S.; Christou, G.; Hendrickson, D. N. *Inorg. Chem.* **1992**, *31*, 1874.
(21) (a) Glowiak, T.; Kubiak, M.; Jesowska-Trzebiatowska, B. *Bull. Acad. Pol. Sci., Sci. Chim.* **1977**, *25*, 359. (b) Cotton, F. A.; Extine, M. W.; Falvello, L. R.; Lewis, D. B.; Lewis, G. E.; Murillo, C. A.; Schwotzer, W.; Tomas, M.; Troup, J. M. *Inorg. Chem.* **1986**, *25*, 3505. (c) Murray, H. H.; Novick, S. G.; Armstrong, W. H.; Day, C. S. *J. Cluster Sci.* **1993**, *4*, 439. (d) Castro, S. L.; Streib, W. E.; Sun, J.-S.; Christou, G. *Inorg. Chem.* **1996**, *35*, 4462.
(22) Robin, M. D.; Day, P. *Adv. Inorg. Chem.* **1967**, *10*, 247.
(23) Harmalker, S. P.; Leparulo, M. A.; Pope, M. T. *J. Am. Chem. Soc.* **1983**, *105*, 4286.
(24) Chakravarty, J.; Dutta, S.; Chakravorty, A. *J. Chem. Soc., Dalton Trans.* **1993**, 2857.
(25) (a) Dean, N. S.; Folting, K.; Lobkovsky, E. B.; Christou, G. *Angew. Chem., Int. Ed. Engl.* **1993**, *32*, 594. (b) Yang, Y.; Liu, Q.; Wu, D. *Inorg. Chim. Acta* **1993**, *208*, 85.
(26) (a) Edema, J. J. H.; Gambarotta, S.; Hao, S.; Bensimon, C. *Inorg. Chem.* **1991**, *30*, 2584. (b) Kang, B.; Weng, L.; Liu, H.; Wu, D.; Huang, L.; Lu, C.; Cai, J.; Chen, X.; Lu, J. *Inorg. Chem.* **1990**, *29*, 4873.

2-mercaptophenol), $[V_3L_2(OH)_2(PO_2(OPh)_2)_4]^+$ and $[V_3L_2(PO_2-(OPh)_2)_6]^+$ (L = hydrotris(pyrazolyl)borate),[27] $[V_3O_2(bdt)_4-(tmeda)_2]^{28}$ (3V^{IV}; bdtH$_2$ = 1,2-benzenedithiol), and the $[V_3O-(P_2O_7)_2]^{29}$ (2V^{III},V^{IV}) repeating unit in the polymer of the same formula.

The magnetochemical studies on **1** and **2**, in conjunction with the EHT calculations, are consistent with both complexes containing a V−V single (σ) bond (d_{z^2}/d_{z^2} overlap). The σ-bonding orbital is low-lying relative to the LUMO ($\sim$0.7 eV, $\sim$5600 cm^{-1}) and effectively ties up two of the four d electrons of **1**. The remaining two d electrons in **1** are distributed among the closely-spaced HOMO and LUMO (0.17 eV from the EHT calculation) to give a singlet ground state and triplet excited state (the single d electron in **2** gives a doublet ground state). The nearest quintet ($S = 2$) state for **1** would additionally necessitate promotion of an electron from the σ-bonding orbital into the SLUMO and thus lies $\sim$2 eV above the ground state and is not thermally populated at room temperature. Complex **1** is thus extremely similar in its electronic structure to $[V_2O(SPh)_4(Me_2bpy)_2]$ (**6**),[10b] and both complexes can be described as possessing a V−V single bond with the remaining two electrons antiferromagnetically coupled *via* a superexchange pathway involving the bridging ligands to give an $S = 0$ ground state and an $S = 1$ excited state. The magnetochemical study on **1** has determined the true singlet−triplet gap to be $|2J| = 838$ cm^{-1}. Note that both **1** and **6** have a V···V separation of $\sim$2.6 Å, consistent with a V−V bond order of 1.

It is important to emphasize, as was done for **6**, that we could ignore the short V−V distance and the EHT calculation and fit the magnetochemical data to a d^2/d^2 system undergoing antiferromagnetic exchange interactions to give an $S = 0, 1, 2$ spin manifold with energies of $0, -2J$, and $-6J$, respectively. This gives equally good fits of the VT χ_M *vs* T data with the same resulting value of J, because the $S = 2$ second excited state would be at $|4J| = 1676$ cm^{-1} above the $S = 1$ state, and thus not populated and irrelevant to the fitting routine. It must, therefore, be appreciated that the magnetochemical analysis of **1** does not itself prove that two electrons are tied up in a σ-bond at all investigated temperatures. However, the availability of magnetochemical data for **2** is crucial to this point, for they show a temperature-independent $S = \frac{1}{2}$ state: if **1** really were an $S = 0, 1, 2$ spin manifold, then **2** should be an $S = \frac{1}{2}, \frac{3}{2}$ spin manifold resulting from exchange interactions between V^{IV} ($S = \frac{1}{2}$) and V^{III} ($S = 1$) ions. The observation of only a single, $S = \frac{1}{2}$, state for **2** supports both the EHT picture of a low-lying σ-bonding orbital and a resulting $S = 0, 1$ spin manifold for **1**. It is interesting to note that $Cp_2V_2(edt)_2^{30a}$ has a quadruply-bridged core similar to that of **1** and a similar V−V distance (2.541(1) Å) and is thus predicted to exhibit a magnetochemical behavior similar to that of **1** and **6**, perhaps even a comparable singlet−triplet gap. *Ab initio* calculations on quadruply-bridged $Cp_2V_2(C_4H_8)_2^{30b}$ yield a picture related to that of **1**, with a similar singlet−triplet gap of 926 cm^{-1}.

The finding of a relatively strong ferromagnetic exchange interaction in **5** was unexpected: there are extremely few previous examples in V^{III} (or V^{IV}) complexes. For V^{III}, other examples include $[L'_2V_2O(O_2CMe)_2]^{2+31}$ ($J > 200$ cm^{-1}; L' = 1,4,7-trimethyl-1,4,7-triazacyclononane)), $[L'_2V_2O(acac)_2]^{2+32}$ ($J = +112$ cm^{-1}), $[V_4O_2(O_2CEt)_7(bpy)_2]^{+33}$ ($J = 27.5$ cm^{-1}, $J' = -31.2$ cm^{-1}), $[L_2V_2O(O_2CEt)_2]^{34}$ ($J > 200$ cm^{-1}; L = hydrotris(pyrazolyl)borate), and $[L_2V_2O(O_2P(OC_6H_5)_2)_2]^{34}$ ($J > 200$ cm^{-1}). $Cs_3V_2Cl_9$ ($J = 5.5$ cm^{-1}) and $Rb_3V_2Cl_9$ ($J = 2.6$ cm^{-1}) are also reported[35] to be ferromagnetic, but crystal structures are not available; $(NEt_4)[V_2Cl_7(THF)_2]^{18}$ ($J = -48$ cm^{-1}) and $(NEt_4)_3[V_2Cl_9]^{36}$ ($J \approx -40$ cm^{-1}) are both antiferromagnetically coupled.

It is of interest to attempt to rationalize the rare occurrence of ferromagnetic coupling in **5** between adjacent V^{III} (d^2) ions. In a series of dinuclear face-sharing bioctahedra of d^3/d^3 ions (V^{II}, Cr^{III}, Mn^{IV}), the coupling was found to be antiferromagnetic in every case, and it was concluded that the magnitude of the coupling was dependent *only* on the M···M separation[37] with direct overlap of the d_π magnetic orbitals being the sole pathway of magnetic exchange. Direct overlap cannot be even the primary pathway in **5**, as that would give a negative J value, and significant superexchange contributions *via* the bridging S atoms must therefore be present.

The magnetic orbitals are all of π symmetry, and it is instructive to consider the inter-metal orbital overlaps that can occur. Consider first a dinuclear V−X−V unit: as has been discussed by Hotzelmann *et al.*,[38] the major superexchange pathways between octahedral metal atoms when only d_π orbitals are half-filled are

V_π	Sp_1	V_π		V_π	Sp_2	V_σ
	antiferromagnetic				ferromagnetic	
	a				**b**	
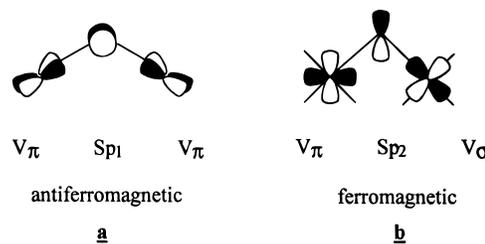
Situation **a** results in antiferromagnetic contributions if both V_π orbitals are half-filled and ferromagnetic if one is empty; situation **b** gives ferromagnetic contributions if d_σ orbitals are empty. In a d^2/d^2 pair, only four of the six d_π orbitals are half-filled, so situation **a** could provide both types of contributions; nevertheless, remembering that the observed J (J_{obs}) is a sum of ferromagnetic (J_F) and antiferromagnetic (J_{AF}) contributions (eq 12), and that antiferromagnetic contributions tend to

$$J_{obs} = J_F + J_{AF} \qquad (12)$$

dominate, one can predict that face-sharing $[X_3M(\mu-X)_3MX_3]$ bioctahedra for d^2/d^2 systems would be expected to be antiferromagnetically-coupled, as found for $(NEt_4)_3[V_2Cl_9]^{36}$ and $(NEt_4)[V_2Cl_7(THF)_2]^{18}$.

(27) Dean, N. S.; Mokry, L. M.; Bond, M. R.; O'Connor, C. J.; Carrano, C. J. *Inorg. Chem.* **1996**, *35*, 3541.
(28) Tsagkalidis, W.; Rodewald, D.; Rehder, D. *J. Chem. Soc., Chem. Commun.* **1995**, 165.
(29) Johnson, J. W.; Johnston, D. C.; King, H. E., Jr.; Halbert, T. R.; Brody, J. F.; Goshorn, D. P. *Inorg. Chem.* **1988**, *27*, 1646.
(30) (a) Rajan, O. A.; McKenna, M.; Noordik, J.; Haltiwanger, R. C.; Dubois, M. K. *Organometallics* **1984**, *3*, 831. (b) Poumbga, C.; Daniel, C.; Benard, M. *Inorg. Chem.* **1990**, *29*, 2387.
(31) Knopp, P.; Wieghardt, K. *Inorg. Chem.* **1991**, *30*, 4061.
(32) Knopp, P.; Wieghardt, K.; Nuber, B.; Weiss, J.; Sheldrick, W. S. *Inorg. Chem.* **1990**, *29*, 363.
(33) Castro, S. L.; Sun, Z.; Bollinger, J. C.; Hendrickson, D. N.; Christou, G. *J. Chem. Soc., Chem. Commun.* **1995**, 2517.
(34) Bond, M. R.; Czernuszewicz, R. S.; Dave, B. C.; Yan, Q.; Mohan, M.; Verastegue, R.; Carrano, C. J. *Inorg. Chem.* **1995**, *34*, 5857.
(35) Leuenberger, B.; Briat, B.; Canit, J. C.; Furrer, A.; Fischer, P.; Güdel, H. U. *Inorg. Chem.* **1986**, *25*, 2930.
(36) Casey, A. T.; Clark, R. J. H. *Inorg. Chem.* **1968**, *7*, 1598.
(37) Niemann, A.; Bossek, U.; Wieghardt, K.; Butzlaff, C.; Trautwein, A. X.; Nuber, B. *Angew. Chem., Int. Ed. Engl.* **1992**, *31*, 311.
(38) Hotzelmann, R.; Wieghardt, K.; Flörke, U.; Haupt, H.-J.; Weatherburn, D. C.; Bonvoisin, J.; Blondin, G.; Girerd, J.-J. *J. Am. Chem. Soc.* **1992**, *114*, 1681.

Why, then, is **5** ferromagnetically coupled? We believe that the answer is that the bridges are RS^- rather than O^{2-}, S^{2-}, or Cl^-. Thus, the bridging S atoms are three-coordinate and distinctly trigonal pyramidal with the sum-of-angles at each S all <300°. The S−C bond strongly stabilizes the S p_1 orbital and effectively shuts down the (predominantly antiferromagnetic) exchange *via* pathway **a**: pathway **b** is still operative, and assuming other antiferromagnetic contributions from direct overlap of d_π orbitals are small, the ferromagnetic contributions from **b** dominate and the observed J_{obs} is positive. Note that the acute (~80°) V−S−V angles serve to increase Sp/Vσ overlap in **b** and hence the J_F contributions to J_{obs}. In essence, the proposed rationalization for the positive J_{obs} value is that the latter arises from ferromagnetic contributions from the several possible "crossed-pathway" overlaps between half-filled d_π and empty d_σ metal orbitals. The weak, antiferromagnetic J' interaction in **5** is less easy to rationalize, but it is close to zero and likely the sum of several weak J_F and J_{AF} contributions.

The EPR spectrum of **2** was not a simple isotropic 15-line signal. Instead, the VT spectra show evidence for a class II system with intermetal electron hopping that is slow on the EPR time scale and with an isotropic eight-line signal at 260 K and an anisotropic signal at 77 K, both typical of *mononuclear* V^{IV} systems. Further study of this species would benefit from, among other things, a low-temperature crystal structure of **1** to assess the degree of structural difference between the halves of the molecule.

Supporting Information Available: Textual and tabular summaries of the structure determinations, tables of atomic coordinates, thermal parameters, and bond distances and angles, and figures with atom numbering for **3**·CH_2Cl_2 and **5**·MeCN (28 pages). Ordering information is given on any current masthead page.

IC9606901